

Phase noise of electro-optic dual frequency combs

CALLUM DEAKIN^{1,*}, ZICHUAN ZHOU¹, AND ZHIXIN LIU¹

¹Department of Electronic and Electrical Engineering, University College London, London, U.K.

*Corresponding author: callum.deakin.17@ucl.ac.uk

Compiled February 4, 2021

Dual frequency combs are emerging as new tools for spectroscopy and signal processing. The relative phase noise of the tone pairs determines the performance (e.g. signal to noise ratio) of the detected spectral components. Although previous research has shown that the signal quality generally degrades with the increase of frequency difference between tone pairs, the scaling of the relative phase noise of dual frequency comb systems has not been fully characterized. In this paper, we model and characterize the phase noise of a coherent electro-optic dual frequency comb system. Our results show that at high offset frequencies, the phase noise is an incoherent sum of the timing phase noise of the two combs, multiplied by line number. At low offset frequencies, however, the phase noise scales more slowly due to the coherence of the common frequency reference. © 2021 Optical Society of America

<http://dx.doi.org/10.1364/ao.XX.XXXXXX>

Dual optical frequency combs have emerged as a useful tool in spectroscopy, where the beating between two frequency combs of different repetition rates can downconvert the broadband optical response of a sample to narrowband radio frequency (RF) signals for ease of processing and analysis [1]. In addition, many have explored adapting the dual frequency comb technique for the signal processing of broadband RF signals [2–4], which is a perennial challenge in wireless and optical communications, radar systems and defense technologies.

In RF signal processing, the dual frequency comb technique effectively acts as a channelizer, spectrally slicing a broadband signal into many narrow band signals that can be processed by a bank of low speed receivers. This channelization allows for high frequency signals to be processed in parallel by multiple low speed receivers, reducing the bandwidth requirements of the receiver sub-components such as filters, analog to digital converters, and digital signal processors. The reduced bandwidth requirement also allows for signal detection and digitization with higher signal to noise ratio (e.g. higher photodiode responsivity), increasing the accuracy of full signal detection. Dual frequency combs have been utilized in this way for photonic assisted analog to digital conversion [5–7], OFDM reception [8], sub-noise compressive signal detection [9, 10], and wideband disambiguation of sparse signals [11].

In contrast to spectroscopy applications, where the frequency

comb sources are typically low repetition rate mode locked lasers, RF signal processors require large (i.e. >10 GHz) comb spacing. Potential comb sources for such applications include electro-optic (modulator based) combs [12], integrated mode locked lasers [13], parametric combs [14] and micro resonators [15]. Electro optic combs offer flexibility of tuning the frequency spacing, high optical power per comb line and can operate over a wide temperature range (e.g. 0–60 °C). Although the tone spacing is conventionally limited to < 50 GHz due to the modulator bandwidth, the availability of high bandwidth and low V_π phase and intensity modulator on the thin-film LiNbO₃ platform could potentially offer >100 GHz tone spacing [16, 17]. Furthermore, expanding the bandwidth of electro-optic combs can be achieved through parametric mixing [18].

When designing any RF signal processor, understanding and minimizing the additive noise of the processor is critical to preserving signal fidelity. At high frequencies, the phase noise (or timing jitter) is particularly important since any timing error will induce noise whose power grows quadratically with frequency. Although the phase noise of electro-optic frequency comb sources is well understood, there is to our knowledge no experimental reports of how this phase noise manifests itself in a dual frequency comb system.

In this paper, we characterize the phase noise of a dual frequency comb system based on electro optic modulator combs synthesized from a common reference. We show that the phase noise power spectrum primarily follows the uncorrelated sum of the RF driving signals, scaled by the square of the comb line number. However, at low offset frequencies, the phase noise scales differently due to correlation between the two frequency combs. In this regime the phase noise follows the reference oscillator phase noise, scaled to the offset frequency between the two combs. Our results highlight that effective design of the RF synthesizers is critical to minimizing the additive phase noise of the dual frequency comb signal processor. In particular, ensuring a high degree of phase noise correlation between the combs (e.g. through a large loop bandwidth phase locked loop) must be balanced with maintaining low absolute phase noise on the individual combs.

As shown in Fig. 1(a), dual frequency combs exploit the Vernier effect in the frequency domain, using two frequency combs of line spacing f_{sig} and $f_{LO} = f_{sig} + \Delta f$. In spectroscopy (Fig. 1(b)), the signal comb is passed through the sample of interest and mixed with the local oscillator (LO) comb on a single photodiode to retrieve the absorption spectrum as a downconverted RF signal. This concept has been adapted for RF signal

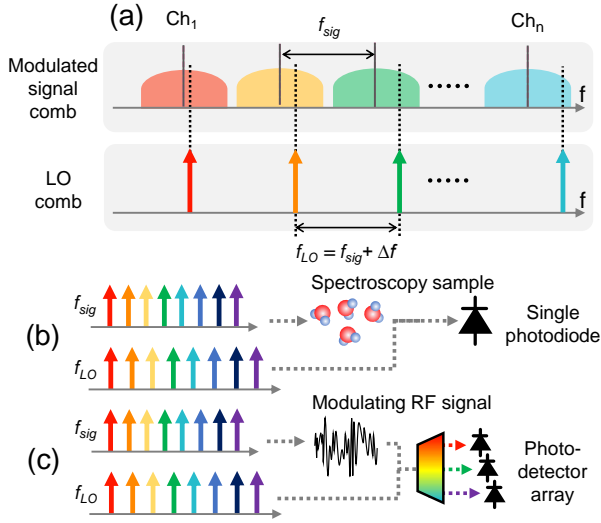


Fig. 1. (a) The Vernier effect in the frequency domain between two combs of spacing f_{sig} and f_{LO} is the key concept in dual comb techniques. This has been applied in (b) spectroscopy and (c) RF signal processing.

processing (Fig. 1(c)) where the signal comb of spacing f_{sig} is modulated by an input RF signal of maximum frequency $f_{sig}/2$ such that the input signal is copied onto every comb line. Following this, comb lines from both combs are separated by arrayed waveguide gratings (AWGs) or other means and fed to a bank of optical coherent receivers. The n -th comb line of the local oscillator (LO) comb therefore acts as a local oscillator to the n -th comb line of the signal comb, offset from the baseband by $n\Delta f$. Each channel is then filtered by a low pass filter of bandwidth $\Delta f/2$, effectively channelizing the broadband input signal into N channels of Δf bandwidth. Application specific digitization and analog/digital signal processing can then follow, all operating at a fraction f_{sig}/N of the original input bandwidth.

As discussed in our theoretical analysis in [19], three main stochastic noise sources can degrade the input signal fidelity during this channelization process: laser noise (including any optical amplifiers), noise added during the comb generation process, and photodiode noise. In this paper, we focus on the impact of phase noise, which consists of both the laser phase noise $\phi_0(t)$ and the phase noise added during the comb generation $\phi_{sig}(t)$ and $\phi_{LO}(t)$. For electro-optic frequency combs the phase noise on the n -th comb line of the signal and LO comb is given by

$$\phi_{sig,total}(t) = \phi_0(t) + n\phi_{sig}(t) \quad (1)$$

$$\phi_{LO,total}(t) = \phi_0(t) + n\phi_{LO}(t) \quad (2)$$

respectively [20–22]. The laser phase noise $\phi_0(t)$ will be canceled at the coherent receiver assuming that optical path length difference between the two combs is significantly shorter than the coherence length of the seed laser. This is trivial to achieve on an integrated platform or with a low linewidth laser, or both.

Thus the phase noise (or timing error) imparted on each channel will be determined purely by the relative timing error between the two frequency combs. If the individual timing errors $\phi_{sig}(t)$ and $\phi_{LO}(t)$ are completely uncorrelated, then the power of the phase noise added on the n -th channel is a simple incoherent sum of the two phase noises

$$S_{u,n}(\omega) = n^2|\phi_{sig}(\omega)|^2 + n^2|\phi_{LO}(\omega)|^2. \quad (3)$$

In electro-optic combs however, when the driving signals are referenced to a common reference, the timing errors are not completely independent. The phase noise of this common reference will be scaled up within the phase lock loop (PLL) and contributes to the overall phase noise of the PLL output signal.

At low offset frequencies, the reference phase noise will dominate the overall phase noise of the PLL. At higher offset frequencies, the phase frequency detector (PFD) and charge pump will tend to contribute the majority of phase noise within the loop bandwidth, with the voltage controlled oscillator (VCO) noise dominating outside the loop bandwidth. For the purposes of this paper, it is useful therefore to separate the common, correlated sources of phase noise (i.e. the reference oscillator) from the separate, uncorrelated sources (PFD, charge pump, VCO)

$$\phi_{sig}(\omega) = k_{sig}(\omega)\phi_c(\omega) + \phi_{u,sig}(\omega) \quad (4)$$

$$\phi_{LO}(\omega) = k_{LO}(\omega)\phi_c(\omega) + \phi_{u,LO}(\omega) \quad (5)$$

where $k_{sig}(\omega)$ and $k_{LO}(\omega)$ are functions describing the mapping of the reference phase noise to the output of the PLL [23]. For example, for a perfect frequency doubler this would simply be $k = 2$. In a PLL, however, this will typically be a complex frequency dependent function describing the phase and amplitude transforms applied by the loop filter, as well as any other mismatches between the two synthesizers. This description leads to a total relative phase noise power in the n -th channel of

$$S_{\Delta\phi_n}(\omega) = n^2 \left[|k_{LO}(\omega) - k_{sig}(\omega)|^2 |\phi_c(\omega)|^2 + |\phi_{u,LO}(\omega)|^2 + |\phi_{u,sig}(\omega)|^2 \right]. \quad (6)$$

What (6) shows is that the total additive phase noise of the dual comb system is not only dependent on the absolute phase noise of each frequency comb, but also the level of correlated and uncorrelated phase noise between each comb and their relationship described by $k_{LO}(\omega) - k_{sig}(\omega)$. This is discussed in more detail in [19].

To measure the phase noise of an electro-optic dual comb system, we devised the experimental setup shown in Fig. 2. A low linewidth (5 kHz) fiber laser at 1555 nm followed by a booster erbium doped fiber amplifier (EDFA) is used to seed two electro-optic frequency comb generators based on cascaded intensity and phase modulators [24]. The comb driving signals were generated from a 100 MHz crystal oscillator reference by two fractional-N PLL based synthesizers (Texas Instruments LMX2595) with an approximate loop bandwidth of 285 kHz and doubled to create two driving signals of frequency 25 GHz and 26 GHz for the signal and LO comb respectively. These driving signals are amplified such that each comb generates approximately 25 comb lines each within 3 dB power variation.

The comb outputs are then mixed in a 50/50 coupler with the coupler outputs being used as the inputs to a 50 Ω loaded 42 GHz optical balanced detector (u2t BPDV2050R). Before being fed to the balanced detector, each branch is filtered by an optical bandpass filter in order to select the n -th comb line, such that a $n\Delta f$ beating signal is observed at the balanced detector output. The phase noise of this beating signal can then be measured by a phase noise analyser (Rohde and Schwarz FSVA3030), with the phase noise averaged over multiple measurements. All optical devices are fiber coupled to polarization maintaining fiber and the power into the photodiode remains constant between measurements. For comparison, we also measured the phase noise of each PLL, $|\phi_{LO}|^2$ and $|\phi_{sig}|^2$, and estimated the expected

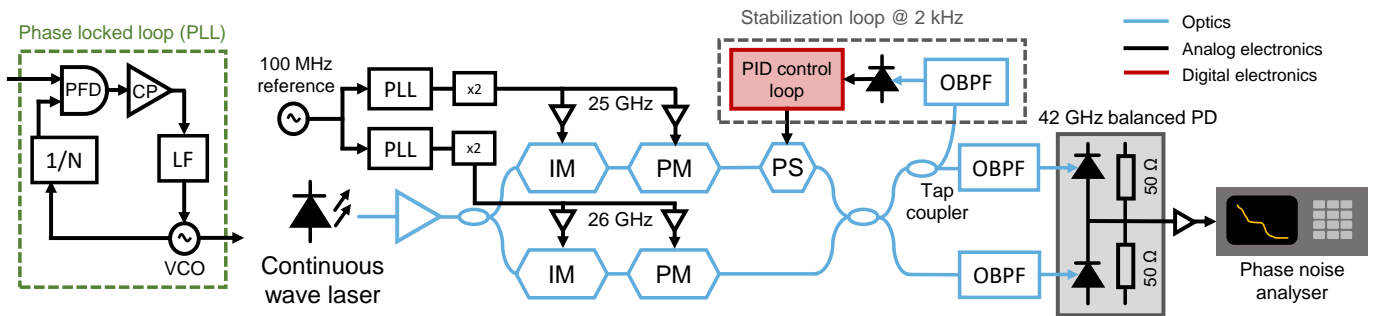


Fig. 2. Experimental setup. IM, intensity modulator; PM, phase modulator; OBPF, optical bandpass filter; PD, photodiode; PS, phase shifter; PID, proportional integral derivative; PFD, phase frequency detector; CP, charge pump; LF, loop filter; VCO, voltage controlled oscillator.

phase noise resulting from a coherent and incoherent sum of their phase noise.

One practical issue with the experimental setup is that the configuration of the two frequency combs essentially acts as a fiber Mach-Zehnder interferometer. Thus, any time dependent vibration and temperature induced phase fluctuations between the two branches will induce slow phase drift that increases the low frequency phase noise measured at the balanced receiver. To mitigate this, we use a slow feedback control loop to compensate for the vibration and thermal induced phase variations. As shown in Fig. 2, a tap coupler is used to tap off 1% of the light in one of the branches after the 50/50 coupler and filtered using an optical bandpass filter such that only the central comb lines are incident on a photodiode. This beating signal between the center tones of the two combs is used as the error signal for a digital proportional integral derivative (PID) controller that is used to stabilize the optical path length variation between the two combs by driving a piezo electric fiber phase shifter.

The PID feedback loop operates at 2 kHz bandwidth and so is able to effectively suppress any sub-kHz temperature and vibration induced optical path length fluctuations between the two branches. It is important to note that this feedback loop is unable to correct for any relative phase noise induced by the frequency combs themselves, since the central tone of the combs does not carry any phase noise from the driving signals (i.e. $n = 0$ in (1)/(2)). The feedback loop therefore only corrects for phase noise induced by the optical path length variation, and allows for accurate measurement of the relative phase noise between the two combs without artificially suppressing the phase noise in the sub-kHz offset frequency region.

In Fig. 3, we use the phase noise measurement of the 10 GHz beat note ($n = 10$ channel) as an example to explain the composition of phase noise of the dual comb system. The measured single side band phase noise is shown as the purple curve, along with the estimated coherent ($n^2|\phi_{LO} - \phi_{sig}|^2$, green curve) and incoherent ($n^2|\phi_{LO}|^2 + n^2|\phi_{sig}|^2$, orange curve) sum of the two driving signals' phase noise. In addition, the $1/f^3$ estimate for the reference phase noise contribution is plotted twice: based on whether the reference phase noise is correlated (green dotted line) or uncorrelated (pink dashed line) between the two comb driving signals. This estimate is derived from a direct measurement of the reference oscillator phase noise.

For frequencies >2 kHz, the phase noise closely follows the incoherent sum of the driving signals phase noise, with the observed phase noise being a result of the incoherent summation

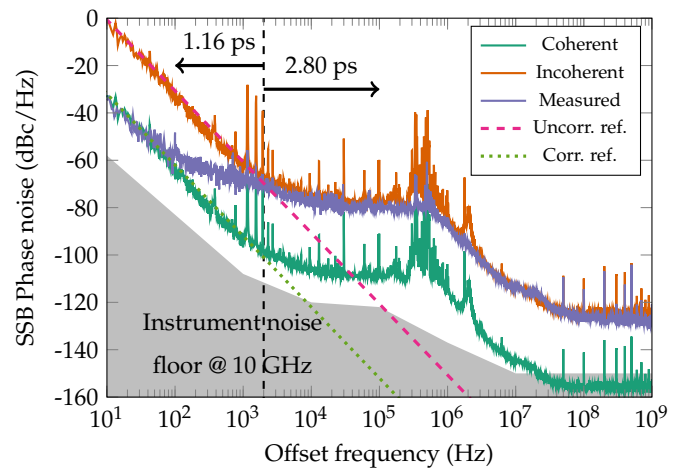


Fig. 3. Measured single side band phase noise of the 10 GHz beat note, whose total integrated jitter is 3.03 ps. Plotted for comparison are the coherent ($n^2|\phi_{LO} - \phi_{sig}|^2$) and incoherent ($n^2|\phi_{LO}|^2 + n^2|\phi_{sig}|^2$) summations of the PLL synthesizers phase noise, along with the integrated jitter above (1.16 ps) and below (2.80 ps) 2 kHz offset. The grey shaded region indicates the phase noise analyser phase noise at 10 GHz.

of the PLL and VCO phase noise ($n^2|\phi_{LO}|^2 + n^2|\phi_{sig}|^2$). The integrated jitter in this section is 2.80 ps. In the low frequency region <2 kHz, however, the main phase noise contribution on each comb is the reference oscillator, which is correlated between the two combs. The phase noise power therefore drops below that predicted by an incoherent summation of the two synthesizers' phase noise, and begins to track the coherent summation of reference phase noise ($n^2|\phi_{LO} - \phi_{sig}|^2$) at approximately <100 Hz. In this section the integrated jitter is 1.16 ps, leading to an overall integrated jitter of 3.03 ps from 10 Hz to 1 GHz, or 0.19 rad at 10 GHz. The exact frequencies of these crossover points will be dependent on the specific reference oscillator used and PLL configuration. Note that the spurs plotted are specific to this system due to the cross talk on the printed circuit board of the PLL synthesizer, and can be eliminated through more careful design of the synthesizer. We suspect that some of these spurs are amplitude noise spurs (e.g. spurs at ≈ 400 kHz) that are suppressed during the nonlinear comb generation process, evi-

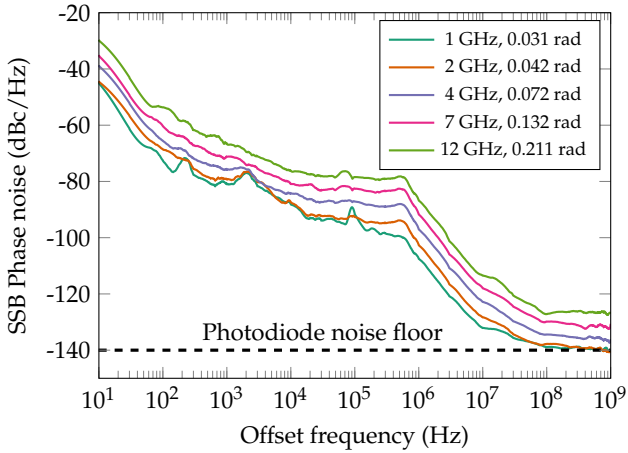


Fig. 4. Measured single side band phase noise of for various comb line numbers, with integrated phase noise from 10 Hz to 1 GHz shown in the legend. The measured phase noise has been smoothed with spurs removed for clarity.

denced by the fact that they do not appear in the measured comb phase noise. However, they appear in the coherent/incoherent estimates due to the limitations of our phase noise analyzer in suppressing amplitude noise during direct measurement of the synthesizers' phase noise.

To show the scaling of phase noise with regard to the beat frequencies, we plot the phase noise for various channel numbers in Fig. 4, i.e. the beating between the n -th comb line of each comb, generating a tone of frequency $n\Delta f$. This shows that the relationship shown in Fig. 3 holds for any channel number. As expected, the total phase noise power increases as n^2 . At low channel numbers (specifically $n = 1, 2$ in Fig. 4), we observed some increase in phase noise in the 2 kHz to 10 kHz region. This is likely the aforementioned vibrations picked up by the experimental setup that were unable to be compensated by the 2-kHz feedback loop, since it does not scale with channel number. This could be reduced by employing a faster feedback loop or photonic integration of the dual comb system. Furthermore, the $n = 1, 2$ channels also reach the photodiode thermal noise floor of our setup at frequencies > 10 MHz.

The results in Fig. 3 and Fig. 4 confirm the description in (6). Furthermore, since in this case the reference noise contribution is negligible above approximately 2 kHz we can write

$$|k_{LO}(\omega) - k_{sig}(\omega)|^2 |\phi_c(\omega)|^2 \approx \left(\frac{\Delta f}{f_{ref}}\right)^2 |\phi_{ref}(\omega)|^2 \quad (7)$$

where $|\phi_{ref}(\omega)|^2$ is the phase noise power of the reference at frequency f_{ref} . This approximation holds for electro-optic dual combs synthesized from a common reference, but may not hold if the reference contributes substantial phase noise at higher offset frequencies, or is not coherent between the two combs.

We have characterized the phase noise measurements of a dual frequency comb system based on electro-optic frequency combs synthesized from a common reference. We show that the phase noise power in the n -th broadly follows the incoherent summation of the two comb driving signals scaled by n^2 . At low offset frequencies however, phase noise correlations between the common reference oscillators results in a coherent sum of the phase noise on each frequency comb and subsequent reduction in the phase noise power. These results can be applied

to estimate the overall performance of a given channelizer, as discussed in [19].

Acknowledgements. The authors thank Prof Enrico Rubiola and Prof Paul Brennan for helpful discussions, and Prof Izzat Darweezah for loan of the phase noise analyser.

Funding. EPSRC grant (EP/R041792/1), EPSRC programme grant TRANSNET (EP/R035342/1), Royal Society Paul Instrument Fund (PIF/R1/180001).

Disclosures. The authors declare no conflicts of interest.

REFERENCES

1. I. Coddington, N. Newbury, and W. Swann, *Optica* **3**, 414 (2016).
2. X. Xie, Y. Dai, K. Xu, J. Niu, R. Wang, L. Yan, and J. Lin, *IEEE Photonics J.* **4**, 1196 (2012).
3. A. Wiberg, D. Esman, L. Liu, J. Adleman, S. Zlatanovic, V. Ataie, E. Myslivets, B. P.-P. Kuo, N. Alic, E. Jacobs *et al.*, *J. Light. Technol.* **32**, 3609 (2014).
4. A. Klee, C. Middleton, and R. DeSalvo, "Dual-comb spectrometer for fast wideband RF spectral analysis," in *2017 IEEE Photonics Conference (IPC)*, (IEEE, 2017), p. WA1.1.
5. C. Deakin and Z. Liu, *Opt. Lett.* **45**, 173 (2020).
6. C. Deakin, T. Odedeyi, and Z. Liu, "Dual frequency comb photonic analog to digital conversion," in *2020 IEEE Photonics Society Summer Topicals Meeting Series (SUM)*, (IEEE, 2020), p. WB4.3.
7. A. Lukashchuk, J. Riemensberger, J. Liu, P. Marin-Palomo, M. Karpov, C. Koos, R. Bouchand, and T. J. Kippenberg, "Photonic-assisted analog-to-digital conversion using integrated soliton microcombs," in *45th European Conference on Optical Communication (ECOC 2019)*, (2019), p. Th.2.E.6.
8. H. Hu, V. Ataie, E. Myslivets, and S. Radic, *J. Light. Technol.* **37**, 1280 (2019).
9. V. Ataie, D. Esman, B. P.-P. Kuo, N. Alic, and S. Radic, *Science* **350**, 1343 (2015).
10. D. J. Esman, V. Ataie, B. P. Kuo, E. Temprana, N. Alic, and S. Radic, *J. Light. Technol.* **34**, 5669 (2016).
11. M. S. Alshaykh, J. D. McKinney, and A. M. Weiner, *IEEE Photonics Technol. Lett.* **31**, 1874 (2019).
12. A. Parriaux, K. Hammani, and G. Millot, *Adv. Opt. Photonics* **12**, 223 (2020).
13. M. L. Davenport, S. Liu, and J. E. Bowers, *Photonics Res.* **6**, 468 (2018).
14. B. P.-P. Kuo, E. Myslivets, V. Ataie, E. G. Temprana, N. Alic, and S. Radic, *J. lightwave technology* **31**, 3414 (2013).
15. A. Pasquazi, M. Peccianti, L. Razzari, D. J. Moss, S. Coen, M. Erkintalo, Y. K. Chembo, T. Hansson, S. Wabnitz, P. DelHaye *et al.*, *Phys. Reports* **729**, 1 (2018).
16. C. Wang, M. Zhang, X. Chen, M. Bertrand, A. Shams-Ansari, S. Chandrasekhar, P. Winzer, and M. Loncar, *Nature* **562**, 101 (2018).
17. M. He, M. Xu, Y. Ren, J. Jian, Z. Ruan, Y. Xu, S. Gao, S. Sun, X. Wen, L. Zhou *et al.*, *Nat. Photonics* **13**, 359 (2019).
18. Z. Tong, A. O. Wiberg, E. Myslivets, B. P. Kuo, N. Alic, and S. Radic, *Opt. Express* **20**, 17610 (2012).
19. C. Deakin and Z. Liu, *Opt. Express* **28**, 39750 (2020).
20. A. Ishizawa, T. Nishikawa, A. Mizutori, H. Takara, A. Takada, T. Sogawa, and M. Koga, *Opt. express* **21**, 29186 (2013).
21. L. Lundberg, M. Mazur, A. Fällö, V. Torres-Company, M. Karlsson, and P. A. Andrekson, "Phase correlation between lines of electro-optical frequency combs," in *CLEO: Science and Innovations*, (Optical Society of America, 2018), p. JW2A.149.
22. G. Brajato, L. Lundberg, V. Torres-Company, M. Karlsson, and D. Zibar, *Opt. express* **28**, 13949 (2020).
23. D. Rönnow, S. Amin, M. Alizadeh, and E. Zenteno, *IET Sci. Meas. & Technol.* **11**, 77 (2017).
24. V. Torres-Company, J. Lancis, and P. Andrés, *Opt. letters* **33**, 1822 (2008).

FULL REFERENCES

1. I. Coddington, N. Newbury, and W. Swann, "Dual-comb spectroscopy," *Optica* **3**, 414 (2016).
2. X. Xie, Y. Dai, K. Xu, J. Niu, R. Wang, L. Yan, and J. Lin, "Broadband photonic rf channelization based on coherent optical frequency combs and i/q demodulators," *IEEE Photonics J.* **4**, 1196–1202 (2012).
3. A. Wiberg, D. Esman, L. Liu, J. Adleman, S. Zlatanovic, V. Ataie, E. Myslivets, B. P.-P. Kuo, N. Alic, E. Jacobs *et al.*, "Coherent filterless wideband microwave/millimeter-wave channelizer based on broadband parametric mixers," *J. Light. Technol.* **32**, 3609–3617 (2014).
4. A. Klee, C. Middleton, and R. DeSalvo, "Dual-comb spectrometer for fast wideband RF spectral analysis," in *2017 IEEE Photonics Conference (IPC)*, (IEEE, 2017), p. WA1.1.
5. C. Deakin and Z. Liu, "Dual frequency comb assisted analog-to-digital conversion," *Opt. Lett.* **45**, 173–176 (2020).
6. C. Deakin, T. Odedeyi, and Z. Liu, "Dual frequency comb photonic analog to digital conversion," in *2020 IEEE Photonics Society Summer Topicals Meeting Series (SUM)*, (IEEE, 2020), p. WB4.3.
7. A. Lukashchuk, J. Riemensberger, J. Liu, P. Marin-Palomo, M. Karpov, C. Koos, R. Bouchand, and T. J. Kippenberg, "Photonic-assisted analog-to-digital conversion using integrated soliton microcombs," in *45th European Conference on Optical Communication (ECOC 2019)*, (2019), p. Th.2.E.6.
8. H. Hu, V. Ataie, E. Myslivets, and S. Radic, "Optical comb assisted ofdm rf receiver," *J. Light. Technol.* **37**, 1280–1287 (2019).
9. V. Ataie, D. Esman, B. P.-P. Kuo, N. Alic, and S. Radic, "Subnoise detection of a fast random event," *Science* **350**, 1343–1346 (2015).
10. D. J. Esman, V. Ataie, B. P. Kuo, E. Temprana, N. Alic, and S. Radic, "Detection of Fast Transient Events in a Noisy Background," *J. Light. Technol.* **34**, 5669–5674 (2016).
11. M. S. Alshaykh, J. D. McKinney, and A. M. Weiner, "Radio-frequency signal processing using optical frequency combs," *IEEE Photonics Technol. Lett.* **31**, 1874–1877 (2019).
12. A. Parriaux, K. Hammani, and G. Millot, "Electro-optic frequency combs," *Adv. Opt. Photonics* **12**, 223–287 (2020).
13. M. L. Davenport, S. Liu, and J. E. Bowers, "Integrated heterogeneous silicon/iii-v mode-locked lasers," *Photonics Res.* **6**, 468–478 (2018).
14. B. P.-P. Kuo, E. Myslivets, V. Ataie, E. G. Temprana, N. Alic, and S. Radic, "Wideband parametric frequency comb as coherent optical carrier," *J. lightwave technology* **31**, 3414–3419 (2013).
15. A. Pasquazi, M. Peccianti, L. Razzari, D. J. Moss, S. Coen, M. Erkintalo, Y. K. Chembo, T. Hansson, S. Wabnitz, P. DelHaye *et al.*, "Micro-combs: A novel generation of optical sources," *Phys. Reports* **729**, 1–81 (2018).
16. C. Wang, M. Zhang, X. Chen, M. Bertrand, A. Shams-Ansari, S. Chandrasekhar, P. Winzer, and M. Lončar, "Integrated lithium niobate electro-optic modulators operating at cmos-compatible voltages," *Nature* **562**, 101–104 (2018).
17. M. He, M. Xu, Y. Ren, J. Jian, Z. Ruan, Y. Xu, S. Gao, S. Sun, X. Wen, L. Zhou *et al.*, "High-performance hybrid silicon and lithium niobate mach-zehnder modulators for 100 gbit s⁻¹ and beyond," *Nat. Photonics* **13**, 359–364 (2019).
18. Z. Tong, A. O. Wiberg, E. Myslivets, B. P. Kuo, N. Alic, and S. Radic, "Spectral linewidth preservation in parametric frequency combs seeded by dual pumps," *Opt. Express* **20**, 17610–17619 (2012).
19. C. Deakin and Z. Liu, "Noise and distortion analysis of dual frequency comb photonic rf channelizers," *Opt. Express* **28**, 39750–39769 (2020).
20. A. Ishizawa, T. Nishikawa, A. Mizutori, H. Takara, A. Takada, T. Sogawa, and M. Koga, "Phase-noise characteristics of a 25-ghz-spaced optical frequency comb based on a phase-and intensity-modulated laser," *Opt. express* **21**, 29186–29194 (2013).
21. L. Lundberg, M. Mazur, A. Fiilöp, V. Torres-Company, M. Karlsson, and P. A. Andrekson, "Phase correlation between lines of electro-optical frequency combs," in *CLEO: Science and Innovations*, (Optical Society of America, 2018), p. JW2A.149.
22. G. Brajato, L. Lundberg, V. Torres-Company, M. Karlsson, and D. Zibar, "Bayesian filtering framework for noise characterization of frequency combs," *Opt. express* **28**, 13949–13964 (2020).
23. D. Rönnow, S. Amin, M. Alizadeh, and E. Zenteno, "Phase noise coherence of two continuous wave radio frequency signals of different frequency," *IET Sci. Meas. & Technol.* **11**, 77–85 (2017).
24. V. Torres-Company, J. Lancis, and P. Andrés, "Lossless equalization of frequency combs," *Opt. letters* **33**, 1822–1824 (2008).